



Research paper

Enhancement of premature stop codon readthrough in the CFTR gene by Ataluren (PTC124) derivatives



Ivana Pibiri ^{a, b, 1}, Laura Lentini ^{a, 1}, Raffaella Melfi ^a, Giulia Gallucci ^a, Andrea Pace ^{a, b, *}, Angelo Spinello ^a, Giampaolo Barone ^{a, b}, Aldo Di Leonardo ^{a, c, **}

^a Dipartimento di Scienze e Tecnologie Biologiche, Chimiche e Farmaceutiche (STEBICEF), Università degli Studi di Palermo, Viale delle Scienze Ed. 17, 90128 Palermo, Italy

^b Istituto EuroMediterraneo di Scienza e Tecnologia (IEMEST), Via Emérico Amari 123, 90139 Palermo, Italy

^c Centro di OncoBiologia Sperimentale (COBS), Via San Lorenzo Colli, 90145 Palermo, Italy

ARTICLE INFO

Article history:

Received 16 March 2015

Received in revised form

14 June 2015

Accepted 19 June 2015

Available online 21 June 2015

Keywords:

Cystic fibrosis

PTCs readthrough

CFTR gene

Green fluorescent protein

Nonsense mutation

Fluorinated oxadiazole

ABSTRACT

Premature stop codons are the result of nonsense mutations occurring within the coding sequence of a gene. These mutations lead to the synthesis of a truncated protein and are responsible for several genetic diseases. A potential pharmacological approach to treat these diseases is to promote the translational readthrough of premature stop codons by small molecules aiming to restore the full-length protein. The compound PTC124 (Ataluren) was reported to promote the readthrough of the premature UGA stop codon, although its activity was questioned. The potential interaction of PTC124 with mutated mRNA was recently suggested by molecular dynamics (MD) studies highlighting the importance of H-bonding and stacking π - π interactions. To improve the readthrough activity we changed the fluorine number and position in the PTC124 fluoroaryl moiety. The readthrough ability of these PTC124 derivatives was tested in human cells harboring reporter plasmids with premature stop codons in H2BGF and Fluc genes as well as in cystic fibrosis (CF) IB3.1 cells with a nonsense mutation. Maintaining low toxicity, three of these molecules showed higher efficacy than PTC124 in the readthrough of the UGA premature stop codon and in recovering the expression of the CFTR protein in IB3.1 cells from cystic fibrosis patient. Molecular dynamics simulations performed with mutated CFTR mRNA fragments and active or inactive derivatives are in agreement with the suggested interaction of PTC124 with mRNA.

© 2015 Elsevier Masson SAS. All rights reserved.

1. Introduction

Nonsense mutations are single nucleotide changes in the gene that result in in-frame UGA (opal), UAG (amber), and UAA (ochre) premature termination codons (PTCs) in the coding region of the mRNA. These PTCs cause inappropriate termination of translation leading to a truncated protein unable to fulfill its functions, and promote mRNA destabilization by the nonsense-mediated mRNA decay (NMD) pathway [1]. Over the years, several strategies have been suggested to facilitate the readthrough of PTCs [2–4], thus restoring the synthesis of a full-length protein. Duchenne muscular

dystrophy and cystic fibrosis are genetic diseases for which these approaches have been tested. Cystic fibrosis (CF) is caused by mutations in the gene encoding the cystic fibrosis transmembrane conductance regulator (CFTR). More than 2000 disease-causing mutations in CFTR have been identified and can be divided into six major classes [5]. The most commonly observed mutations include three base pair deletion causing the loss of phenylalanine at position 508 (Δ F508), a missense mutation at position 551 and a nonsense mutation at position 542 (G542X) known as a class I mutation type. Generally, CF patients with nonsense-mutation in the CFTR gene produce no CFTR protein thus suffering from a more severe form of the disease. A potential treatment for these patients is to selectively promote translational readthrough of the PTC so that the expression of a functional protein will be restored to some extent. To this aim aminoglycosides antibiotics (gentamicin, tobramycin, paromomycin, geneticin etc.) were previously employed to suppress the normal proof-reading function of the ribosome [6,7] leading to the insertion of a near-cognate amino acid

* Corresponding author. Dipartimento di Scienze e Tecnologie Biologiche, Chimiche e Farmaceutiche (STEBICEF), Università degli Studi di Palermo, Viale delle Scienze Ed. 16, 90128 Palermo, Italy.

** Corresponding author. Centro di OncoBiologia Sperimentale (COBS) via San Lorenzo Colli 90145 Palermo, Italy.

E-mail addresses: andrea.pace@unipa.it (A. Pace), aldo.dileonardo@unipa.it (A. Di Leonardo).

¹ I.P. and L.L.: these authors contributed equally to this study.

at the PTC site, thus allowing the translation of the remainder of the open reading frame. This “translational readthrough” of premature stop codons, but not of normal termination codons, has been shown to partially restore protein function in a number of pre-clinical settings [8–10]. However, severe side-effects caused by prolonged treatments with aminoglycosides including renal, auditory, and vestibular toxicities have been reported [11], along with the reduced read-through ability at subtoxic doses in a mouse model [12] and in clinical trials [13]. These results have limited the widespread clinical use of aminoglycosides for this purpose. The compound PTC124, also known as Ataluren, was originally reported to promote the readthrough of premature but not normal termination co-dons in HEK293 cells transfected with a luciferase reporter gene (LUC190) harboring a PTC at Thr190, where the normal ACA codon was replaced with either UAA, UAG, or UGA codon [14]. PTC124 does not possess the toxicity of an aminoglycoside and has been suggested as a potential treatment of genetic disorders caused by nonsense mutations, particularly those involving the UGA premature codon [12,14,15]. Although earlier studies [16–19] questioned whether Ataluren promoted readthrough, this issue has now been addressed by other independent publications demonstrating this compound's readthrough activity in diverse cellular and animal models [20–26]. In this context of contrasting results, obtained from both *in vitro* and *in vivo* experiments, PTC124's mechanism of action still remains not well established [4]. Therefore, it is crucial that claims regarding the readthrough activity of PTC124 or of its derivatives are confirmed by experiments on at least two reporters (orthogonal assay) [27,28]. In our previous study, we attempted to rationalize PTC124's high selectivity toward the readthrough of *opal* with respect to *amber* and *ochre* nonsense mutations. Computational results on the hypothesized supramolecular interaction between PTC124 and mRNA highlighted that a selective interaction with the premature UGA codon occurs through hydrogen bonding of PTC124 carboxylic moiety and stacking interactions involving its aromatic rings. On this basis, we were prompted to investigate variations of the PTC124 scaffold, particularly considering the esterification of the carboxylic moiety as well as the number and position of fluorine atoms as factors able to strongly affect the PTC124's ability to interact with its biological target. These modifications, some of which were previously pointed out by PTC Therapeutics [29], would allow us to focus our biological assays to rationalize structure-activity relationships (SAR). Synthesized derivatives were first tested for their readthrough activity with a luciferase-based reporter. Most active compounds were further tested with a green fluorescent protein (GFP) based reporter and evaluated for the suppression of nonsense mutations in the CFTR gene in the human bronchial epithelial cell line IB3.1 (CFTR genotype W1282X/F508del).

2. Materials and methods

2.1. Chemistry

IR spectra were registered with a Shimadzu FTIR-8300 instrument. ^1H NMR of all compounds and ^{13}C NMR spectra of representative **4a** and **5b,i** were recorded on a Bruker 300 Avance spectrometer, operating at the indicated frequency, with TMS as an internal standard. Flash chromatography was performed by using silica gel (Merck, 0.040–0.063 mm) and mixtures of ethyl acetate and petroleum ether (fraction boiling in the range of 40–60 °C) in various ratios. GC–MS determinations were carried out on a Shimadzu GCMS-QP2010 system. All solvents and reagents were obtained from commercial sources. All synthesized compounds were purified by chromatography and analyzed by IR, GC–MS and NMR. Purity of synthesized compounds was verified prior to biological

tests by HPLC and NMR. In all the cases purity was higher than 95%. HRMS spectra were recorded by analyzing a 50 ppm solution of the compound in a 6540 UHD Accurate-Mass Q-TOF LC/MS (Agilent Technologies) equipped with a Dual AJS ESI source.

2.1.1. General procedure for the synthesis of compounds **3** and **4a–l**

2 mmol of either amidoxime **1** [30] or **2** [26] were dissolved in acetone (200 mL) in a round-bottomed flask; then, K_2CO_3 (0.35 g; 2.5 mmol) and the corresponding aryl chloride (2.5 mmol), were added to the reaction mixture and stirred for 24 h at room temperature. The solvent was removed under vacuum and the residue treated with water and refluxed for 30 min. 1,2,4-Oxadiazoles products were obtained by filtration and further purified by chromatography.

2.1.1.1. 3-Toluyyl, 5-(2-fluorophenyl)-1,2,4-oxadiazole (3a). Yield 70%; m.p. 93–95 °C (lit. 93 °C) [31]. HRMS for $\text{C}_{15}\text{H}_{11}\text{FN}_2\text{O}$ found 255.0924 $[\text{M}+\text{H}]^+$ (Calcd 255.0928).

2.1.1.2. Methyl 3-(5-(2-fluorophenyl)-1,2,4-oxadiazol-3-yl)benzoate (4a). Yield 80%; m.p. 134–136 °C; IR (nujol): 1723 cm^{-1} ; ^1H NMR (300 MHz, CDCl_3): δ (ppm) 8.78 (m, 1H), 8.31 (m, 1H), 8.18 – 8.12 (m, 2H), 7.59 – 7.52 (m, 2H), 7.32 – 7.20 (m, 2H), 3.91 (s, 3H). ^{13}C NMR (75 MHz, CDCl_3): δ (ppm) 173.8, 168.8, 167.0, 163.6, 159.4, 149.6, 135.4, 132.9, 132.4, 131.7, 129.6, 127.9, 125.4, 117.9, 115.0, 53.0. GC–MS: m/z (%) 298 (M^+ , 60), 267(70), 177 (35), 146 (60), 130 (100), 102 (60), 75 (45), 44 (75). HRMS for $\text{C}_{16}\text{H}_{11}\text{FN}_2\text{O}_3$ found 299.0817 $[\text{M}+\text{H}]^+$ (Calcd 299.0826).

2.1.1.3. Methyl 3-(5-(3-fluorophenyl)-1,2,4-oxadiazol-3-yl)benzoate (4b). Yield 78%; m.p. 124–126 °C; IR (nujol): 1733 cm^{-1} ; ^1H NMR (300 MHz, CDCl_3): δ (ppm) 8.84 (s, 1H), 8.37 (d, 1H, $J = 7.2$ Hz), 8.21 (d, 1H, $J = 8.4$ Hz), 8.04 (d, 1H, $J = 6.9$ Hz), 7.94 (d, 1H, $J = 9$ Hz), 7.64 – 7.53 (m, 2H), 7.37 – 7.26 (m, 1H), 3.99 (s, 3H). GC–MS: m/z (%) 298 (M^+ , 60), 267(90), 177 (25), 146 (65), 130 (100), 102 (60), 75 (45), 44 (60). HRMS for $\text{C}_{16}\text{H}_{11}\text{FN}_2\text{O}_3$ found 299.0823 $[\text{M}+\text{H}]^+$ (Calcd 299.0826).

2.1.1.4. Methyl 3-(5-(4-fluorophenyl)-1,2,4-oxadiazol-3-yl)benzoate (4c). Yield 86%; m.p. 164–166 °C; IR (nujol): 1733 cm^{-1} ; ^1H NMR (300 MHz, CDCl_3): δ (ppm) 8.84 (m, 1H), 8.36 (m, 1H), 8.28 – 8.19 (m, 3H), 7.64 – 7.58 (m, 1H), 7.29 – 7.23 (m, 2H), 3.98 (s, 3H). GC–MS: m/z (%) 298 (M^+ , 80), 267(100), 177 (35), 146 (80), 130 (85), 102 (55), 88 (40), 75 (50). HRMS for $\text{C}_{16}\text{H}_{11}\text{FN}_2\text{O}_3$ found 299.0812 $[\text{M}+\text{H}]^+$ (Calcd 299.0826).

2.1.1.5. Methyl 3-(5-(2,3-difluorophenyl)-1,2,4-oxadiazol-3-yl)benzoate (4d). Yield 82%; m.p. 146–148 °C; IR (nujol): 1722 cm^{-1} ; ^1H NMR (300 MHz, CDCl_3): δ (ppm) 8.85 (m, 1H), 8.38 (m, 1H), 8.22 (m, 1H), 8.04 – 7.99 (m, 1H), 7.63 (m, 1H), 7.47 – 7.44 (m, 1H), 7.32 – 7.26 (m, 1H), 3.98 (s, 3H). GC–MS: m/z (%) 316 (M^+ , 70), 285(100), 146 (60), 130 (45), 113 (30), 102 (40), 88 (30). HRMS for $\text{C}_{16}\text{H}_{10}\text{F}_2\text{N}_2\text{O}_3$ found 317.0723 $[\text{M}+\text{H}]^+$ (Calcd 317.0732).

2.1.1.6. Methyl 3-(5-(2,4-difluorophenyl)-1,2,4-oxadiazol-3-yl)benzoate (4e). Yield 92%; m.p. 126–128 °C; IR (nujol): 1730 cm^{-1} ; ^1H NMR (300 MHz, CDCl_3): δ (ppm) 8.84 (s, 1H), 8.26 – 8.20 (m, 3H), 7.61 (m, 1H), 7.14 – 7.02 (m, 2H), 3.98 (s, 3H). GC–MS: m/z (%) 316 (M^+ , 55), 285(65), 177 (30), 139 (60), 130 (100), 113 (30), 102 (65), 88 (40), 75 (40). HRMS for $\text{C}_{16}\text{H}_{10}\text{F}_2\text{N}_2\text{O}_3$ found 317.0719 $[\text{M}+\text{H}]^+$ (Calcd 317.0732).

2.1.1.7. Methyl 3-(5-(2,5-difluorophenyl)-1,2,4-oxadiazol-3-yl)benzoate (4f). Yield 78%; m.p. 161–163 °C; IR (nujol): 1714 cm^{-1} ; ^1H NMR (300 MHz, CDCl_3): δ (ppm) 8.84 (s, 1H), 8.38 (m, 1H), 8.22 (m,

1H), 7.98 – 7.93 (m, 1H), 7.62 (m, 1H), 7.34 – 7.27 (m, 2H), 3.99 (s, 3H). GC–MS: m/z (%) 316 (M+, 65), 285 (100), 146 (60), 130 (70), 113 (30), 102 (40), 88 (30), 75 (25). HRMS for C₁₆H₁₀F₂N₂O₃ found 317.0724 [M+H]⁺ (Calcd 317.0732).

2.1.1.8. Methyl 3-(5-(2,6-difluorophenyl)-1,2,4-oxadiazol-3-yl)benzoate (4g). Yield 88%; m.p. 136–138 °C; IR (nujol): 1734 cm⁻¹; ¹H NMR (300 MHz, CDCl₃): δ (ppm) 8.84 (m, 1H), 8.40 – 8.37 (m, 1H), 8.23 – 8.20 (m, 1H), 7.64 – 7.59 (m, 2H), 7.14 (m, 2H), 3.97 (s, 3H). GC–MS: m/z (%) 316 (M+, 40), 285 (60), 177 (30), 139 (65), 130 (100), 102 (60), 88 (40), 75 (40). HRMS for C₁₆H₁₀F₂N₂O₃ found 317.0721 [M+H]⁺ (Calcd 317.0732).

2.1.1.9. Methyl 3-(5-(3,4-difluorophenyl)-1,2,4-oxadiazol-3-yl)benzoate (4h). Yield 79%; m.p. 145–147 °C; IR (nujol): 1728 cm⁻¹; ¹H NMR (300 MHz, CDCl₃): δ (ppm) 8.82 (m, 1H), 8.35 (m, 1H), 8.23–8.20 (m, 1H), 8.12 – 8.00 (m, 2H), 7.61 (m, 1H), 7.42 – 7.34 (m, 1H), 3.98 (s, 3H). GC–MS: m/z (%) 316 (M+, 70), 285 (90), 161 (45), 139 (65), 130 (100), 113 (50), 102 (60), 88 (45), 75 (50). HRMS for HRMS for C₁₆H₁₀F₂N₂O₃ found 317.0723 [M+H]⁺ (Calcd 317.0732).

2.1.1.10. Methyl 3-(5-(2,4,5-trifluorophenyl)-1,2,4-oxadiazol-3-yl)benzoate (4i). Yield 81%; m.p. 132–134 °C; IR (nujol): 1716 cm⁻¹; ¹H NMR (300 MHz, CDCl₃): δ (ppm) 8.83 (m, 1H), 8.36 (m, 1H), 8.22 (m, 1H), 8.16 – 8.08 (m, 1H), 7.65 – 7.59 (m, 1H), 7.23 – 7.14 (m, 1H), 3.99 (s, 3H). GC–MS: m/z (%) 334 (M+, 55), 303 (60), 159 (50), 146 (60), 130 (100), 102 (45), 88 (45), 75 (40). HRMS for HRMS for C₁₆H₉F₃N₂O₃ found 335.0638 [M+H]⁺ (Calcd 335.0633).

2.1.1.11. Methyl 3-(5-(perfluorophenyl)-1,2,4-oxadiazol-3-yl)benzoate (4l). Yield 83%; m.p. 109–110 °C; IR (nujol): 1725 cm⁻¹; ¹H NMR (300 MHz, CDCl₃): δ (ppm) 8.83 (s, 1H), 8.38 (d, 1H, J = 7.8 Hz), 8.24 (d, 1H, J = 7.8 Hz), 7.64 (m, 1H); GC–MS: m/z (%) 370 (M+, 25), 339 (50), 193 (40), 161 (20), 146 (30), 130 (100), 102 (65), 88 (25), 75 (30), 51 (15), 44 (65). HRMS for HRMS for C₁₆H₇F₅N₂O₃ found 371.0439 [M+H]⁺ (Calcd 371.0449).

2.1.2. General procedure for the synthesis of 5b,i,l

Similarly to what reported for the synthesis of PTC124 **5a** [26], either methylester **4b**, **4i**, or **4l** (0.34 mmol) were dissolved in benzene (40 mL) in a round-bottomed flask; then, BBr₃ (4 mL; 13.7 mmol) was added to the reaction mixture and stirred at 80 °C for 4 h. The solvent was removed under vacuum and the residue treated with water, extracted with ethyl acetate and dried over anhydrous sodium sulphate. After removal of the solvent under vacuum acids **5b**, **5i**, and **5l** were purified by chromatography.

2.1.2.1. 3-(5-(3-Fluorophenyl)-1,2,4-oxadiazol-3-yl)benzoic acid (5b). Yield 70%; m.p. 252–254 °C; IR (nujol): 1698 cm⁻¹; ¹H NMR (300 MHz, DMSO-*d*₆): δ (ppm) 8.61 (s, 1H), 8.31 (d, 1H, J = 7.8 Hz), 8.17 (d, 1H, J = 7.8 Hz), 8.07–7.97 (m, 2H), 7.76 – 7.69 (m, 2H), 7.64 – 7.57 (m, 1H). ¹³C NMR (75 MHz, CDCl₃): δ (ppm) 174.7, 167.9, 166.6, 164.3, 160.4, 132.4, 132.0, 131.1, 129.8, 127.9, 126.5, 125.3, 124.4, 120.5, 114.8. HRMS for C₁₅H₉FN₂O₃ found 285.0662 [M+H]⁺ (Calcd 285.0670).

2.1.2.2. 3-(5-(2,4,5-Trifluorophenyl)-1,2,4-oxadiazol-3-yl)benzoic acid (5i). Yield 70%; m.p. 248–250 °C; IR (nujol): 1685 cm⁻¹; ¹H NMR (300 MHz, DMSO-*d*₆): δ (ppm) 8.69 (s, 1H), 8.47 – 8.37 (m, 2H), 8.24 (d, 1H, J = 7.8 Hz), 8.08 – 8.03 (m, 1H), 7.84 – 7.79 (m, 1H). ¹³C NMR (75 MHz, DMSO-*d*₆): δ (ppm) 171.3, 167.6, 166.7, 158.3, 154.5, 150.7, 144.7, 132.4, 131.0, 129.8, 127.9, 126.2, 118.8, 108.6, 108.2. HRMS for C₁₅H₇F₃N₂O₃ found 320.0399 [M+H]⁺ (Calcd 320.0409).

2.1.2.3. 3-(5-(Perfluorophenyl)-1,2,4-oxadiazol-3-yl)benzoic acid (5l). Yield 78%, m.p. 202–203 °C, IR (nujol): 3250, 1715 cm⁻¹; ¹H NMR (300 MHz, DMSO-*d*₆): δ (ppm) 8.67 (s, 1H), 8.39 (d, 1H, J = 7.8 Hz), 8.25 (d, 1H, J = 7.8 Hz), 7.83 (m, 1H), 6.58 (bs, OH). HRMS for C₁₅H₅F₅N₂O₃ found 357.0285 [M+H]⁺ (Calcd 357.0293).

2.2. Biology

2.2.1. Cell culture conditions and transfection of reporter plasmids

HeLa and IB3.1 cells were cultured in DMEM supplemented with FBS 10% (GIBCO) in a humidified atmosphere of 4% CO₂ in air at 37 °C. HeLa cells plated in a 6 well plate at a density of 2 × 10⁵/mL were transfected with the reporter plasmids by using lipofectamine 2000 (Invitrogen). HeLa stably transfected cells were selected by blasticidin (5 µg/mL) and 15 clones of H2BGFP-*opal*, 5 clones of H2BGFP-*amber* and 2 clones of H2BGFP-*ochre* were isolated. mRNA levels of the H2BGFP mutated genes were verified by Real-Time qRT-PCR (details in [Supplementary Data](#)).

2.2.2. Construction of reporter plasmids by site directed mutagenesis and clone screening

Reporter plasmids harboring PTCs were constructed by using the pBOS-H2BGFP plasmid [32,33]. The tryptophan codon (TGG) at position 1197-9 of the GFP coding sequence was mutagenized to introduce a stop codon (TGA, TAG or TAA). Four clones from each reaction of mutagenesis were screened by “selective PCR” ([Supporting Information](#)). Plasmid DNA from positive clones was purified with NucleoSpin Plasmid miniprep kit (Macherey-Nagel) and the mutations were verified by sequencing (Eurofins MWG Operon).

2.2.3. Genomic DNA purification and reporter gene control

To isolate genomic DNA from the selected clones we used the PureLink Genomic DNA Kit (Invitrogen). 3 × 10⁶ cells were lysed and the DNA was rapidly purified using a spin column based centrifugation procedure. To verify the integrity of the H2BGFP reporter gene 130 ng of genomic DNA were used as template for a PCR reaction. We used the EF1α forward primer annealing to the gene promoter region and the GFP3' reverse primer annealing to the 3' end of the gene. After 35 cycles of amplification 5 µl of PCR product were run on 1% agarose gel.

2.2.4. Measurement of luciferase activity by luminescence

HeLa cells were plated in a 12 well plate at a density of 1 × 10⁵/mL and transfected with WT (Fluc) and mutant (Fluc-*opal*) plasmids, by using lipofectamine 2000 (Invitrogen). Cells were incubated for 24 h and PTC124 (**5a**) and its derivatives (12 µM) were added for 24 h. Next, cells were washed with PBS, incubated with the detection mix Steady-Glo luciferase reagent (Promega) and 200 µl of cell suspension were plated in triplicate in a 96 well. Luciferase activity was measured on a luminometer (Promega). This experiment was performed three times and quantitative data illustrated in [Fig. 1](#) are the average of the repeated experiments.

2.2.5. Immunofluorescence microscopy

To visualize GFP and CFTR proteins cells were grown on rounded glass coverslips and fixed with methanol for 2 min. The cell membrane and Golgi apparatus were stained by the Wheat Germ Agglutinin (WGA) Alexa 594 (Life Technologies). For GFP-detection cells were permeabilized with 0.01% TritonX (Sigma-Aldrich) in PBS (15 min) and blocked with 0.1% BSA (30 min) both at RT. Cover slips were incubated with a mouse monoclonal antibody against GFP (Sigma-Aldrich, 5 µg/mL) and a mouse monoclonal antibody (CF3) that recognizes the first extracellular loop of human CFTR (Abcam, 1:500) overnight at 4 °C, followed by a goat anti-mouse IgG-FITC

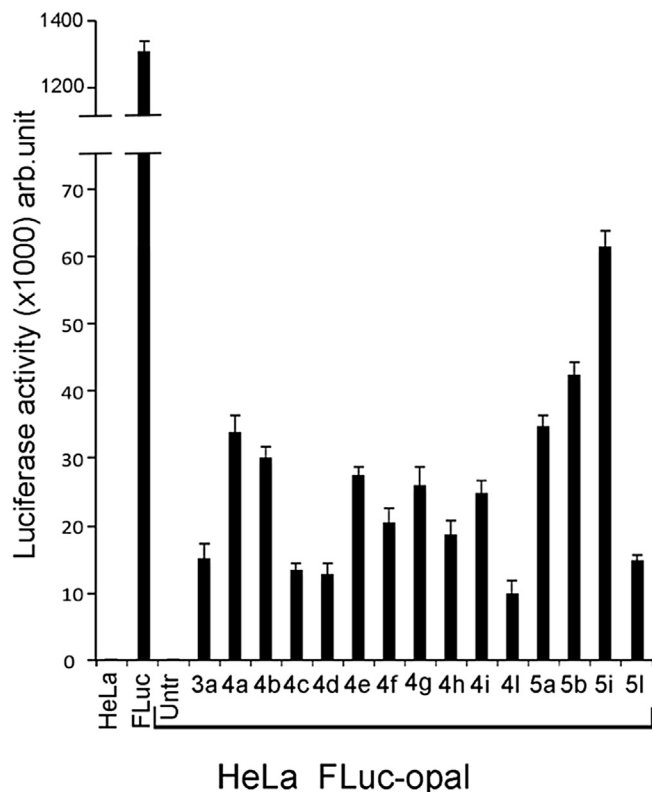


Fig. 1. Luciferase activity after treating HeLa Fluc190^{UGA} transfected cells with PTC124 and its derivatives **3a**, **4** and **5** in comparison with wt Fluc and untransfected or untreated cells (HeLa).

(Sigma-Aldrich, 1:200) and goat polyclonal to mouse Alexa-Fluor-488 (Abcam, 1:1000) secondary antibodies for 1 h at 37 °C. Nuclei were visualized with DAPI. Cells were examined under a Zeiss Axioskop microscope equipped for fluorescence.

2.2.6. Western blotting

Proteins (50 µg) were separated by 10% SDS-PAGE and 4–12% SDS-PAGE (Bolt, Life Technologies) containing 0.1% SDS and transferred to Hybond-C nitrocellulose membranes (Amersham Life Science) by electroblotting [34]. The membrane was incubated with anti-GFP mouse (Sigma-Aldrich, 2 µg/mL), as primary antibody and HRP-conjugated anti-mouse IgG (Abcam, 1:5000), as secondary antibody. For CFTR detection the membrane was incubated with a goat polyclonal antibody anti-CFTR (C-19, Santa Cruz 1:500) raised against a peptide mapping near the C-terminus of CFTR of human origin, and HRP-conjugated anti-goat (Abcam, 1:5000). The target protein was detected by ECL reagents (Pierce). We used β-tubulin antibody (mouse; Sigma-Aldrich 1:10,000) to confirm equal proteins loading. Gel bands were quantified by Image Lab software (BioRad). WB assays were repeated at least three times and were reproducible within 5% variations. Representative WB images and data have been selected for Figs. 3 and 5A.

2.3. Computational details

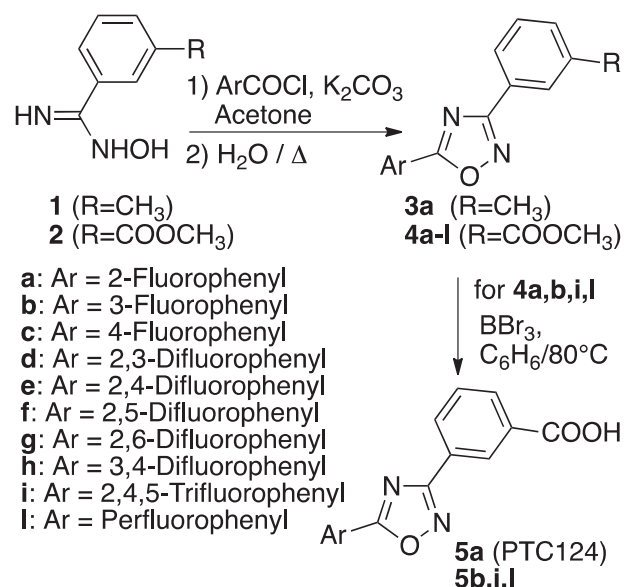
The topology of **5i** and **4d** ligands was generated using ACPYPE [35–37] and Molecular Dynamics (MD) simulations were performed with the GROMACS 4.6.6 suite [38,39] using the AMBER ff99SB force field [40] with parmBsc0 nucleic acid torsions [41]. MD simulations of 50 ns were conducted to assess the supramolecular interactions between the mRNA fragment described above and two

PTC124 derivatives above. The starting position of both ligands was retained from the equilibrium geometry reported for the analogous PTC124-mRNA complex [26]. A cubic box filled with TIP3P water molecules was added around the RNA and the ligand to a depth 0.8 nm on each side of the solute. Na⁺ counterions were added to neutralize the negative charges of the RNA backbone, other Na⁺ and Cl⁻ ions were added to achieve a solution ionic strength of about 0.15 M. Simulations were performed in the NPT ensemble, at the temperature of 300 K. All covalent bonds were constrained with the LINCS algorithm. Energy minimization was run for 5000 steps using the steepest descend algorithm. In a 500 ps equilibration the oligonucleotides were harmonically restrained with a force constant of 1000 kJ mol⁻¹ nm⁻² at 300 K, which was gradually lowered until no restrains were applied. The binding free energy was calculated using the g_mmpbsa [42], with snapshots extracted every 0.5 ns from the production trajectory. Simulations were also conducted mimicking a 9 mM magnesium ion concentration without observing any difference in the interaction between UGA and **5i**.

3. Results

Generally, 1,2,4-oxadiazoles biological activity is related to their bioisosterism with amides and esters [43], and to the H-bond accepting nature of the ring heteroatoms [44]. Recently, the carboxylic moiety of PTC124 has been reported to be involved as H-bond acceptor in relevant snapshots of MD simulation of the selective interaction with the premature UGA codon in a 33-nt long mRNA fragment coding for CFTR [26]. Therefore, by following the amidoxime route for the synthesis of fluoroarylated 1,2,4-oxadiazoles [45–49], we synthesized the corresponding methyl **3a** and methylester **4a** derivatives of PTC124 (Scheme 1) that were tested for readthrough activity with a Fluc-based reporter (Fig. 1).

For the preliminary evaluation of the readthrough activity of compounds **3–5**, we used the FLuc cell-based assay [14,26]. HeLa cells were transiently transfected with the plasmids pFluc-WT and pFluc-*opal*, and FLuc gene expression was measured by luminescence. The dose used (12 µM) was chosen on the basis of our previous results on PTC124 [26]. The three most active compounds **4a**,



Scheme 1. Synthesis of PTC124's derivatives.

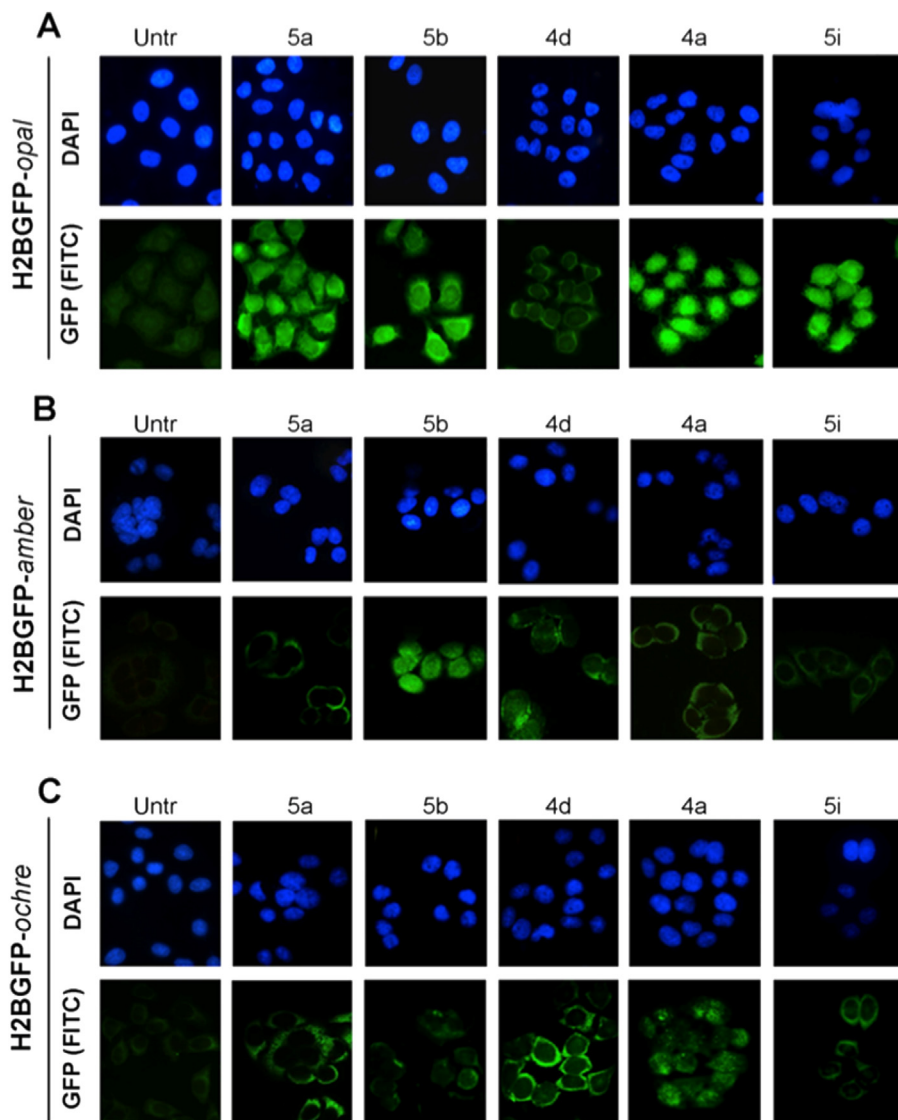


Fig. 2. Immunofluorescence of HeLa cells stably transfected with the H2BGFP-*opal* (A), H2BGFP-*amber* (B) and H2BGFP-*ochre* (C) plasmid untreated (Untr) and treated with the indicated compounds for 24 h. H2BGFP fusion protein (green) was detected with a specific anti-GFP antibody revealed by a FITC-conjugated antibody. Nuclei (blue) were DAPI stained. (For interpretation of the references to color in this figure legend, the reader is referred to the web version of this article.)

5b and **5i** showed readthrough activity also at lower concentrations (3 μ M and 6 μ M) with **5i** showing the higher activity (see Fig. 5 in Supplementary Data). Detection of high levels of luciferase showed by HeLa cells transfected with the pLuc-WT plasmid indicated the correct functioning of this assay.

Despite the absence of the carboxyl moiety, compound **3a** retained some activity, although it was significantly lower compared to PTC124. This suggests that H-bonding from the carboxyl moiety is important but not crucial for activity. Interestingly, the activity of the methylester **4a** was very similar to that of PTC124 thus confirming the role of the carboxyl moiety as H-bond acceptor. Therefore, we focused on the fluoroaryl ring by synthesizing a series of methylester derivatives of PTC124 where the number and the position of fluorine atoms have been varied (Scheme 1). PTC124 **5a** and carboxylic acids **5b,i,l** were obtained by demethylation of the corresponding esters **4a,b,i,l** with boron tribromide.

Luciferase activity data illustrated in Fig. 1 clearly pointed out that in the methylester series the activity is not enhanced by increasing the number of fluorine atoms and that, for

monofluorinated derivatives **4a-c**, the position of fluorine in the ring can cause a dramatic change in activity.

The three most active compounds, ester **4a** and acids **5b** and **5i**, together with the least active ester **4d**, and PTC124 **5a**, were subjected to further evaluation by using a GFP-based assay as previously reported [26]. For this purpose, live cell fluorescence microscopy is not always able to detect low level of H2BGFP re-expression in live cells because of the intrinsic low amount of recoded mRNA by readthrough of premature stop codons [26]. Therefore, to enhance H2BGFP detection, we investigated the readthrough ability of PTC124's derivatives by indirect immunofluorescence analysis in HeLa cells stably transfected with the pBOS-H2BGFP wild-type (wt) plasmid (control) and the *opal*-, *amber*-, and *ochre*-mutated pBOS-H2BGFP plasmids. Immunofluorescence microscopy done in H2BGFP-*opal*-, *amber*-, *ochre* transfected HeLa cells revealed the presence of positive cells for the H2BGFP protein induced by PTC124 and by derivatives **5b**, **4a**, **5i** (Fig. 2) when compared to untreated cells. These immunofluorescence experiments confirmed that the readthrough of the UGA premature stop codon (*opal*) resulted, at least partially, in a

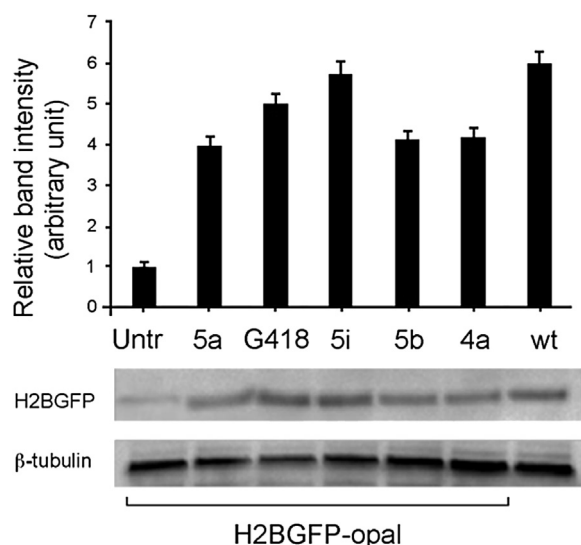


Fig. 3. Western blot showing H2BGFP protein levels in H2BGFP–opal transfected HeLa cells left untreated (untr.) or treated with PTC124 (**5a**), G418 and the indicated PTC124 derivatives. Protein extracts of HeLa H2BGFP-wt cells were used as a control for the H2BGFP-wt protein, β -tubulin was used as a loading control. The histogram below the WB quantitates the Western bands by densitometry by using the Image Lab software (BioRad). A primary antibody targeting the C-terminus of GFP protein was used.

functional protein since the green fluorescence was mainly observed in the nucleus, with compounds **4a** and **5b** showing a brighter green fluorescence (Fig. 2A). Interestingly, cells transfected with the plasmids bearing the UAA (*amber*) stop codon showed some fluorescence when treated with the compound **5b** (Fig. 2B), while treatment with **4a** resulted in weak fluorescence in cells transfected with the plasmid bearing the UAG (*ochre*) stop codon (Fig. 2C). This may suggest that selectivity towards a given PTC could be driven by very small changes in the scaffold structure, although specific readthrough optimization still remains a

distant goal.

These results were confirmed by western blotting analysis that detected a similar amount of full-length H2BGFP protein in HeLa cells transfected with the reporter harboring the premature stop codon and treated with compounds **4a**, and **5b,i**, PTC124, and the known readthrough promoter G418 (Fig. 3).

Since compounds **4a** and **5b,i** performed well in both Fluc and GFP reporters, we tested them for nonsense suppression in CF bronchial epithelial cell line IB3.1 derived from a CF patient (CFTR genotype W1282X/F508del). HT29 cells were used as a positive control for the CFTR protein expression (see Fig. 6 in Supplementary Data). Fluorescence microscopy confirmed that compounds **4a** and **5b,i** were able to readthrough the UGA premature stop codon in IB3.1 cells as showed by the detection of increased level of the CFTR protein (Fig. 4A). Tests performed on compound **4d**, which was the least active with the Fluc and GFP reporters, confirmed its inactivity (data not reported). Comparison of **5i** activity with G418, that is known to do the readthrough of premature stop codons, confirmed this result (Fig. 4B).

To confirm immunofluorescence results we evaluated the CFTR levels in IB3.1 cells by Western blotting (Fig. 5A). The IB3.1 cells were treated with G418, PTC124 (**5a**) and the derivatives **4a**, and **5b,i** for 24 h. Western blot results indicated that the treatment with G418 and PTC124's derivatives induced the recovery of the CFTR protein expression. With respect to the CFTR protein expressed in the untreated cells, data show a five-fold increase for compounds **5i** and **4a** and a sixfold increase for compound **5b**, while PTC124 induced a less pronounced protein recovery (Fig. 5A). Interestingly, ester **4a**, which was chemically stable in the presence of water under neutral conditions, produced a higher level of CFTR protein than its corresponding acid **5a**. However, at this stage we cannot exclude that such activity derives from a higher cell penetration of **4a** followed by its enzymatic hydrolysis into the active acid **5a**. Also, we evaluated the CFTR mRNA levels after the treatment with G418, PTC124 (**5a**), **5i**, **5b**, and **4a**. As shown in Fig. 5B, the mRNA levels in cells treated with G418 were higher than those detected in cells treated with PTC124 and its derivatives, and did not correlate with

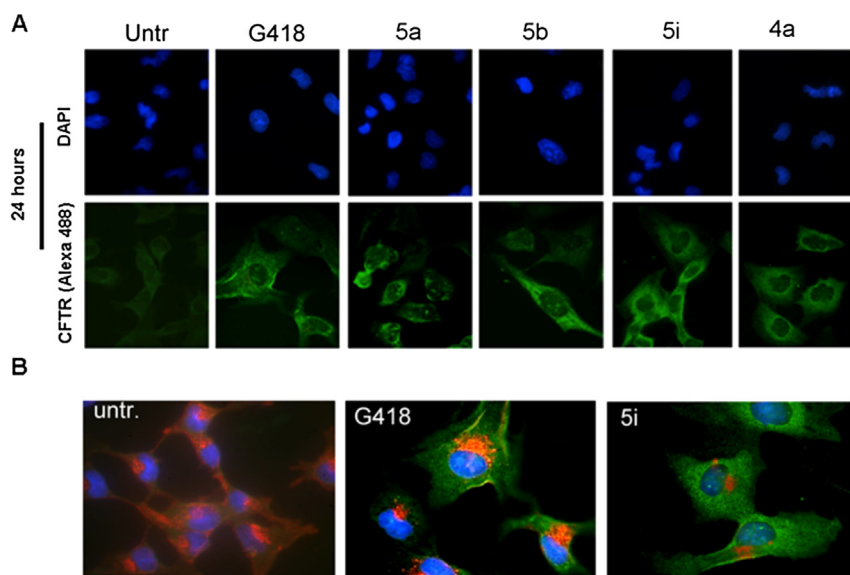


Fig. 4. A) Immunofluorescence assay to detect readthrough of the UGA stop codon in CFTR of IB3.1 human cells untreated (untr.), treated with G418 (positive control) and with PTC124 (**5a**) and its derivatives: **5b**, **5i** and **4a** for 24 h. CFTR protein was revealed by a specific antibody targeting its first external portion (green, Alexa-488). Nuclei (blue) were DAPI stained. B) Cells untreated and treated with G418 and **5i** for 24 h. CFTR protein was revealed by a specific antibody targeting its external portion when located on the membrane (green, Alexa 488). Nuclei (blue) were DAPI stained the cell membrane and Golgi apparatus was stained in red (WGA-Alexa 594). (For interpretation of the references to color in this figure legend, the reader is referred to the web version of this article.)

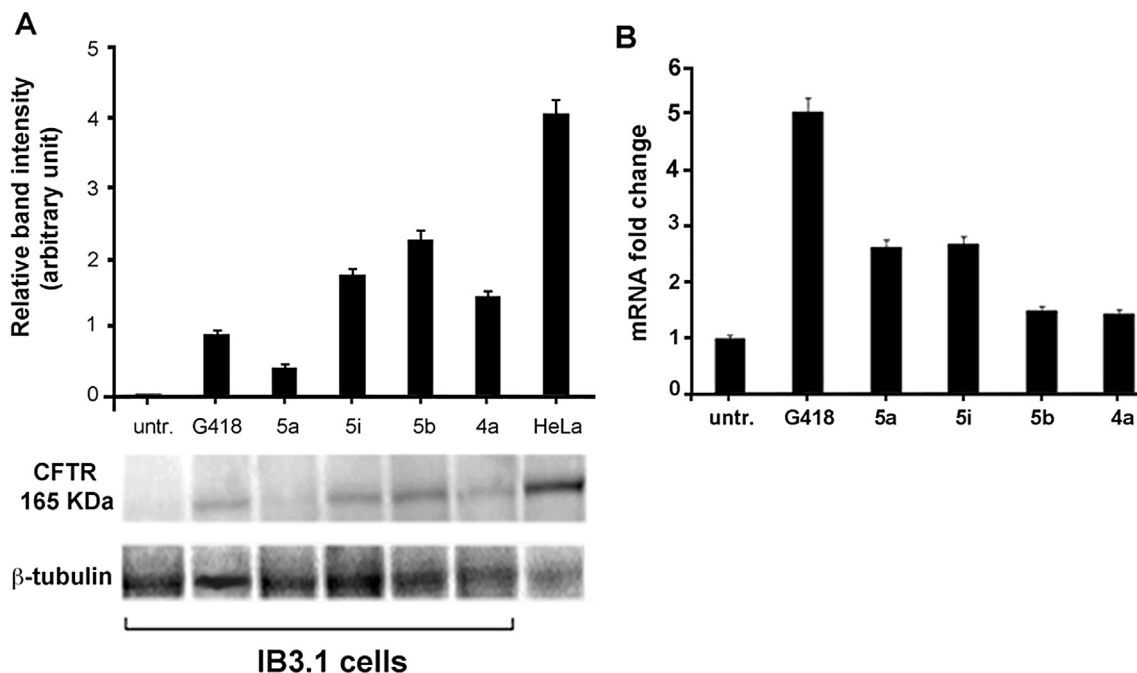


Fig. 5. A) Western blot (bottom panel) showing CFTR protein levels in IB3.1 cells untreated (untr.) or treated with the indicated compounds. HeLa cells were used as a control for the CFTR protein. The upper panel shows the quantitation of the bands by densitometry by using the Image Lab software (BioRad). A primary antibody targeting the C-terminus of CFTR was used, β -tubulin was used as a loading control. B) Real Time RT-PCR showing CFTR mRNA levels in IB3.1 cells untreated (untr.) or treated with the indicated compounds.

the protein levels detected by Western Blot.

Additionally, a cell viability assay was performed to determine if the new molecules affected cell survival. The assay showed that, at the used doses, only G418 resulted toxic for the cells (Fig. 6) while no cytotoxic effects were observed in IB3.1 cells treated for 10 days with both PTC124 and its derivatives (data not shown).

Finally, similarly to our previous study [26] and based on the experimental data obtained in this work with various PTC124 derivatives, we decided to perform a molecular dynamics simulation modeling the interaction of a 33-nucleotides CFTR mRNA fragment, harboring a UGA premature stop codon, with the most active **5i** and the least active, **4d**, derivatives. The trifluorinated derivative, **5i**, was posed in the same orientation of the equilibrium structure of PTC124 [26] and a 50 ns MD simulation was performed. The ligand

remains in the RNA loop for the whole simulation time.

As shown in Fig. 7 (left), there are at least two stabilizing interactions in the **5i**/mRNA complex. Indeed, besides stacking interactions, the occurrence of hydrogen bond between the heterocyclic fluorine atoms and the oxadiazole heterocyclic nitrogen with the amino group on the nucleobases contributes significantly to the complex stability. The binding free energy of the complex between **5i** and the mRNA fragment is -128.1 kJ/mol, similar to that observed for the PTC124/mRNA complex [26]. Interestingly, under the same simulation conditions, inactive compound **4d** readily moves far away from the UGA codon.

4. Discussion

Nonsense mutations are detected in ~10% of Cystic Fibrosis patients representing one of the most severe forms of the disease. A potential therapeutic strategy for these patients is to promote the readthrough of premature stop codons to restore a full length CFTR protein [50]. We used Ataluren as a starting point for selected modifications of moieties possibly involved in its readthrough activity, particularly focusing on the carboxylic moiety, and on the number and relative position of fluorine substituents. In fact, the carboxymethyl moiety could positively influence the absorption process by decreasing the hydrophilicity induced by the carboxylic group. In monofluorinated derivatives, we varied the position of fluorine considering that the electronic demand of the fluorine atom is balanced by the electron-withdrawing feature of the 1,2,4-oxadiazole ring exerted through its C(5) position. These effects can be either counterposed to each other or coupled depending on their relative position. This phenomenon affects the overall polarization of the aromatic rings involved in stacking interactions with the biological target. Finally, due to their strong electronegativity, the introduction of additional fluorine atoms affects the electronic distribution affecting the molecule's lipophilicity that is strictly connected to its pharmacokinetics.

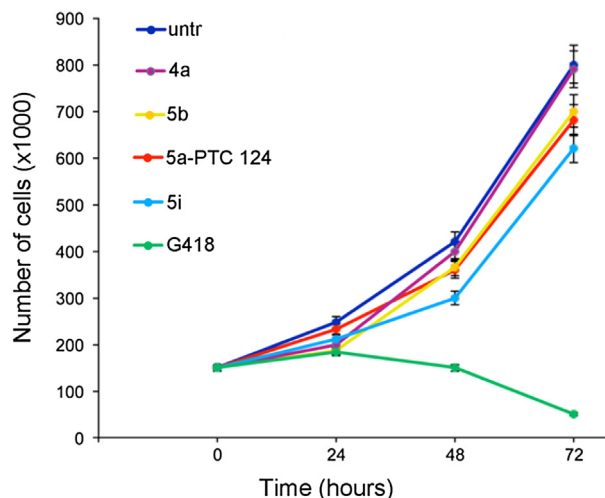


Fig. 6. Cell viability assay shows that only G418 resulted toxic after 72 h of treatment.

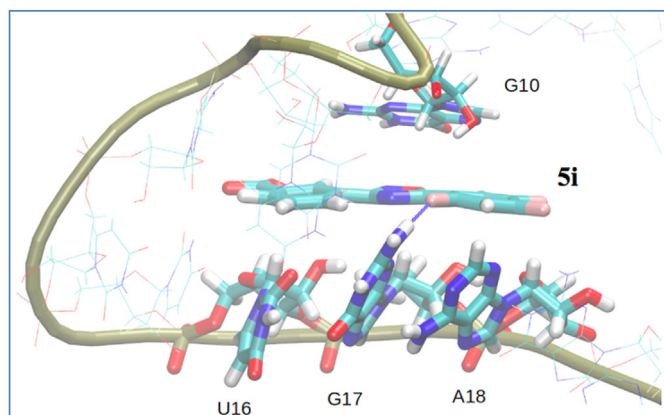


Fig. 7. Representative snapshot showing the interaction of **5i** with the UGA codon. The hydrogen bond between a fluorine atom and the amino group of G17 is evidenced with a blue line. (For interpretation of the references to color in this figure legend, the reader is referred to the web version of this article.)

To validate the efficacy of the synthesized compounds we used orthogonal cell-based assays employing two different reporter systems: the plasmid pBOS-H2BGFP and the luciferase reporter gene (FLuc190) [26]. Indeed, the use of orthogonal assays is considered a powerful approach, which uses different reporters to verify that positive results of a compound's biological activity do not depend on the detection method used [27,28,51,52]. Our immunofluorescence experiments showed that three of the PTC124 derivatives promoted the readthrough of the nonsense mutations present in the H2BGFP reporter plasmid in HeLa transfected cells. The readthrough ability of PTC124's derivatives was confirmed by using an additional assay based on IB3.1 cells derived from a CF patient and harboring a nonsense mutation in the CFTR gene. Treatment of IB3.1 cells with compounds **4a**, **5b**, and **5i** induced the readthrough of the premature translation termination codon encoded by the hCFTR-W1282X nonsense mutation present in these cells, resulting in the partial restoration of the CFTR protein. Real time RT-PCR experiments indicated that there was a lower increase of the CFTR mRNA after the treatment with the PTC124's derivatives in comparison to G418, while Western Blotting experiments showed that the amount of CFTR protein after the treatment with the PTC124's derivatives was greater than that showed by G418 and PTC124 treatment in IB3.1 cells. This last finding reinforces the hypothesis that readthrough, and not stabilization of the protein encoded by the reporter (H2B-GFP-*opal*), is the mechanism responsible for the recoding of the internal TGA premature stop codon. The slight increase (though statistically not significant) in CFTR mRNA observed after treatments also suggests that combining PTC124 derivatives with NMD inhibitors could have a synergistic effect in recovering CFTR.

Finally, we decided to verify if our previous computational approach [26] was able to discriminate between active and inactive compounds. MD simulations were performed with representative active (**5i**) and inactive (**4d**) derivatives in the presence of a 33-bases fragment of the CFTR mRNA sequence containing a premature UGA codon. Interestingly, during the simulation, compound **4d** moves away from its potential UGA target. On the other hand, the simulation reproduced a UGA binding interaction only in the case of active compound **5i** as observed previously for PTC124 [26].

5. Conclusions

Collectively, our results obtained with different experimental approaches imply the readthrough activity of our PTC124

derivatives. It is worth noting that some monofluorinated derivatives of PTC124, differing from our compounds only for the position of the carboxylic moiety on the phenyl ring linked to the C(3) of the 1,2,4-oxadiazole, showed no readthrough activity in a previous SAR study using a luciferase reporter from *Renilla reniformis* (Rluc) [16]. This apparent contrast with our results with Fluc, GFP and CFTR remarks a few important principles that should be considered in the roadmap to nonsense mutation suppressors, especially in a context where the mechanism of action is not established: i) negative results can stem from a fault in any of the three steps of target-reaching, effective target-ligand interaction, measurable effects; ii) both positive and negative results may suffer from specificity towards the experimental setup; iii) indirectly detected readthrough activity (e.g. by fluorimetric methods) should be accompanied by supporting Western Blotting experiments for the specific quantitation of recovered protein; iv) positive results should further be tested for functionality of the recovered protein, e.g. by *in vivo-in vitro* studies; v) ideally, recovered functional proteins should be fully sequenced to identify the type of occurred repair among amino acid skip, substitution, or correct introduction. Importantly, cell viability studies confirmed the lack of toxicity of PTC124's derivatives compared with G418. In our opinion, toxicity data together with the differences in size and shape with aminoglycosides, and the opposite activity of G418 and PTC124 derivatives reported in some cases for the same cellular setup, suggest that PTC124 and its derivatives may not share the same biological target. Unfortunately, while the interaction of G418 with its target is known [8,53], other challenges are still open to understand the mechanism of action of small molecules promoting premature stop codons' readthrough [50]. From a mechanistic point of view, our simulations suggest that mRNA could be one of the possible targets for PTC124-like readthrough promoters. However, neither PTC124 positioning in the ribosomal machinery nor its supposed interaction with mRNA have been experimentally proven and studies in these directions should be encouraged.

Conflict of interest

The authors declare that they have no conflict of interest.

Acknowledgments

We thank Prof. J. Inglese, NIH Chemical Genomics Center, National Institutes of Health, Bethesda, for kindly providing us with the FLuc190^{UGA} plasmid. We are very grateful to Allan Jacobson, University of Massachusetts Medical School, Worcester, for his valuable comments on the manuscript. This work was funded by the Italian Cystic Fibrosis Research Foundation, grant FFC#2/2011, with the contribution of Delegazione di Lecce, Delegazione di Vittoria (Ragusa) to Prof. Aldo Di Leonardo and grant FFC#1/2014 with the contribution of Delegazioni FFC di Palermo, Vittoria (Ragusa) and Catania 2 to Dr. Laura Lentini.

Appendix A. Supplementary data

Supplementary data related to this article can be found at <http://dx.doi.org/10.1016/j.ejmech.2015.06.038>.

References

- [1] S. Kervestin, A. Jacobson, NMD: a multifaceted response to premature translational termination, *Nat. Rev. Mol. Cell. Biol.* 13 (2012) 700–712.
- [2] J.A. Loudon, Cancer: a novel “no-nonsense” approach to treatment, *Oncol. Res.* 19 (2010) 55–66.
- [3] J. Karjolic, I.-T. Yu, Therapeutic suppression of premature termination codons: mechanisms and clinical considerations (Review), *Int. J. Mol. Med.* 34

- (2014) 355–362.
- [4] S.W. Peltz, M. Morsy, E.M. Welch, A. Jacobson, Ataluren as an agent for therapeutic nonsense suppression, *Annu. Rev. Med.* 64 (2013) 407–425.
 - [5] S.M. Rowe, S. Miller, E.J. Sorscher, Cystic fibrosis, *N. Engl. J. Med.* 352 (2005) 1992–2001.
 - [6] J.F. Burke, A.E. Mogg, Suppression of a nonsense mutation in mammalian cells *in vivo* by the aminoglycoside antibiotics G-418 and paromomycin, *Nucleic Acids Res.* 13 (1985) 6265–6272.
 - [7] M. Manuvakhova, K. Keeling, D.M. Bedwell, Aminoglycoside antibiotics mediate context-dependent suppression of termination codons in a mammalian translation system, *RNA* 6 (2000) 1044–1055.
 - [8] T. Hermann, Aminoglycoside antibiotics: old drugs and new therapeutic approaches, *Cell. Mol. Life Sci.* 64 (2007) 1841–1852.
 - [9] K.M. Keeling, D.A. Brooks, J.J. Hopwood, P. Li, J.N. Thompson, D.M. Bedwell, Gentamicin-mediated suppression of Hurler syndrome stop mutations restores a low level of alpha-L-iduronidase activity and reduces lysosomal glycosaminoglycan accumulation, *Hum. Mol. Genet.* 10 (2001) 291–299.
 - [10] D.M. Bedwell, A. Kaenjak, D.J. Benos, Z. Bebok, J.K. Bubien, J. Hong, A. Tousson, J.P. Clancy, E.J. Sorscher, Suppression of a CFTR premature stop mutation in a bronchial epithelial cell line, *Nat. Med.* 3 (1997) 1280–1284.
 - [11] A. Prayle, A.R. Smyth, Aminoglycoside use in cystic fibrosis: therapeutic strategies and toxicity, *Curr. Opin. Pulm. Med.* 16 (2010) 604–610.
 - [12] M. Du, X. Liu, E.M. Welch, S. Hirawat, S.W. Peltz, D.M. Bedwell, PTC124 is an orally bioavailable compound that promotes suppression of the human CFTR-G542X nonsense allele in a CF mouse model, *Proc. Natl. Acad. Sci. U. S. A.* 105 (2008) 2064–2069.
 - [13] E. Kerem, Pharmacologic therapy for stop mutations: how much CFTR activity is enough? *Curr. Opin. Pulm. Med.* 10 (2004) 547–552.
 - [14] E.M. Welch, E.R. Barton, J. Zhuo, Y. Tomizawa, W.J. Friesen, P. Trifillis, S. Paushkin, M. Patel, C.R. Trotta, S. Hwang, R.G. Wilde, G. Karp, J. Takasugi, G. Chen, S. Jones, H. Ren, Y.C. Moon, D. Corson, A.A. Turpoff, J.A. Campbell, M.M. Conn, A. Khan, N.G. Almstead, J. Hedrick, A. Mollin, N. Risher, M. Weetall, S. Yeh, A.A. Branstrom, J.M. Colacino, J. Babiak, W.D. Ju, S. Hirawat, V.J. Northcutt, L.L. Miller, P. Spatrick, F. He, M. Kawana, H. Feng, A. Jacobson, S.W. Peltz, H.L. Sweeney, PTC124 targets genetic disorders caused by nonsense mutations, *Nature* 447 (2007) 87–91.
 - [15] E. Kerem, S. Hirawat, S. Armoni, Y. Yaakov, D. Shoseyov, M. Cohen, M. Nissim-Rafinia, H. Blau, J. Rivlin, M. Aviram, G.L. Elfring, V.J. Northcutt, L.L. Miller, B. Kerem, M. Wilschanski, Effectiveness of PTC124 treatment of cystic fibrosis caused by nonsense mutations: a prospective phase II trial, *Lancet* 372 (2008) 719–727.
 - [16] D.S. Auld, N. Thorne, W.F. Maguire, J. Inglese, Mechanism of PTC124 activity in cell-based luciferase assays of nonsense codon suppression, *Proc. Natl. Acad. Sci. U. S. A.* 106 (2009) 3585–3590.
 - [17] P.K. Dranchak, E. Di Pietro, A. Snowden, N. Oesch, N.E. Braverman, S.J. Steinberg, J.G. Hacia, Nonsense suppressor therapies rescue peroxisome lipid metabolism and assembly in cells from patients with specific PEX gene mutations, *J. Cell. Biochem.* 112 (2011) 1250–1258.
 - [18] S.C. Harmer, J.S. Mohal, D. Kemp, A. Tinker, Readthrough of long-QT syndrome type 1 nonsense mutations rescues function but alters the biophysical properties of the channel, *Biochem. J.* 443 (2012) 635–642.
 - [19] S.P. McElroy, T. Nomura, L.S. Torrie, E. Warbrick, U. Gartner, G. Wood, W.H. McLean, A lack of premature termination codon read-through efficacy of PTC124 (Ataluren) in a diverse array of reporter assays, *PLoS Biol.* 11 (2013) e1001593.
 - [20] C. Sarkar, Z. Zhang, A.B. Mukherjee, Stop codon read-through with PTC124 induces palmitoyl-protein thioesterase-1 activity, reduces thioester load and suppresses apoptosis in cultured cells from INCL patients, *Mol. Genet. Metab.* 104 (2011) 338–345.
 - [21] T. Goldmann, N. Overlack, F. Moller, V. Belakhov, M. van Wyk, T. Baasov, U. Wolftrum, K. Nagel-Wolftrum, A comparative evaluation of NB30, NB54 and PTC124 in translational read-through efficacy for treatment of an USH1C nonsense mutation, *EMBO Mol. Med.* 4 (2012) 1186–1199.
 - [22] Y. Zhou, Q. Jiang, S. Takahagi, C. Shao, J. Uitto, Premature termination codon readthrough in the ABCG6 gene: potential treatment for pseudoxanthoma elasticum, *J. Invest. Dermatol.* 133 (2013) 2672–2677.
 - [23] C. Kuschal, J.J. DiGiovanna, S.G. Khan, R.A. Gatti, K.A. Kraemer, Repair of UV photolesions in xeroderma pigmentosum group C cells induced by translational readthrough of premature termination codons, *Proc. Natl. Acad. Sci. U. S. A.* 110 (2013) 19483–19488.
 - [24] M. Li, M. Andersson-Lendahl, T. Sejersen, A. Arner, Muscle dysfunction and structural defects of dystrophin-null sapje mutant zebrafish larvae are rescued by ataluren treatment, *FASEB J.* 28 (2014) 1593–1599.
 - [25] C.Y. Gregory-Evans, X. Wang, K.M. Wasan, J. Zhao, A.L. Metcalfe, K. Gregory-Evans, Postnatal manipulation of Pax6 dosage reverses congenital tissue malformation defects, *J. Clin. Invest.* 124 (2014) 111–116.
 - [26] L. Lentini, R. Melfi, A. Di Leonardo, A. Spinello, G. Barone, A. Pace, A. Palumbo Piccionello, I. Pibiri, Toward a rationale for the PTC124 (Ataluren) promoted readthrough of premature stop codons: a computational approach and GFP-reporter cell-based assay, *Mol. Pharm.* 11 (2014) 653–664.
 - [27] N. Thorne, D.S. Auld, J. Inglese, Apparent activity in high-throughput screening: origins of compound-dependent assay interference, *Curr. Opin. Chem. Biol.* 14 (2010) 315–324.
 - [28] N. Thorne, J. Inglese, D.S. Auld, Illuminating insights into firefly luciferase and other bioluminescent reporters used in chemical biology, *Chem. Biol.* 17 (2010) 646–657.
 - [29] G.M. Karp, S. Hwang, G. Chen, N.G. Almstead, Y.-C. Moon, 1,2,4-oxadiazole benzoic acid compounds and their use for nonsense suppression and the treatment of disease, *U. S. Pat. Appl. Publ.* 2006 US6992096B2.
 - [30] R.M. Srivastava, M.N. Ramos, L.M. Mendes e Silva, Synthesis, spectroscopic studies and molecular orbital calculations of O-acylbenzamidoximes, *Gazz. Chim. Ital.* 113 (1983) 845–850.
 - [31] P.K. Gupta, M.K. Hussain, M. Asad, R. Kant, R. Mahar, S.K. Shukla, K. Hajela, Metal-free tandem approach to structurally diverse N-heterocycles: synthesis of 1,2,4-oxadiazoles and pyrimidinones, *New J. Chem.* 38 (2014) 3062–3070.
 - [32] T. Kanda, K.F. Sullivan, G.M. Wahl, Histone-GFP fusion protein enables sensitive analysis of chromosome dynamics in living mammalian cells, *Curr. Biol.* 8 (1998) 377–385.
 - [33] L. Lentini, A. Amato, T. Schillaci, L. Insalaco, A. Di Leonardo, Aurora-A transcriptional silencing and vincristine treatment show a synergistic effect in human tumor cells, *Oncol. Res.* 17 (2008) 115–125.
 - [34] C. Ferretti, P. Totta, M. Fiore, M. Mattiuzzo, T. Schillaci, R. Ricordy, A. Di Leonardo, F. Degrassi, Expression of the kinetochore protein Hec1 during the cell cycle in normal and cancer cells and its regulation by the pRb pathway, *Cell Cycle* 9 (2010) 4174–4182.
 - [35] A.W. Sousa Da Silva, W.F. Vranken, E.D. Laue, ACPYPE – Antechamber python parser interface, *BMC Res. Notes* 5 (2012) 367.
 - [36] J.M. Wang, W. Wang, P.A. Kollman, D.A. Case, Automatic atom type and bond type perception in molecular mechanical calculations, *J. Mol. Graph. Model.* 25 (2006) 247–260.
 - [37] J.M. Wang, R.M. Wolf, J.W. Caldwell, P.A. Kollman, D.A. Case, Development and testing of a general amber force field, *J. Comput. Chem.* 25 (2004) 1157–1174.
 - [38] B. Hess, C. Kutzner, D. van der Spoel, E. Lindahl, GROMACS 4: algorithms for highly efficient, load-balanced, and scalable molecular simulation, *J. Chem. Theory Comput.* 4 (2008) 435–447.
 - [39] D. Van der Spoel, E. Lindahl, B. Hess, G. Groenhof, A.E. Mark, H.J.C. Berendsen, GROMACS: fast, flexible, and free, *J. Comput. Chem.* 26 (2005) 1701–1718.
 - [40] A. Perez, I. Marchan, D. Svozil, J. Sponer, T.E. Cheatham, C.A. Loughton, M. Orozco, Refinement of the AMBER force field for nucleic acids: improving the description of alpha/gamma conformers, *Biophys. J.* 92 (2007) 3817–3829.
 - [41] A.T. Guy, T.J. Piggot, S. Khalid, Single-stranded DNA within nanopores: conformational dynamics and implications for sequencing: a molecular dynamics simulation study, *Biophys. J.* 103 (2012) 1028–1036.
 - [42] R. Kumari, R. Kumar, Open Source Drug Discovery Consortium; Lynn, A. g_mmpbsa – a GROMACS tool for high-throughput MM-PBSA calculations, *J. Chem. Inf. Model.* 54 (2014) 1951–1962.
 - [43] A. Pace, P. Pierro, The new era of 1,2,4-oxadiazoles, *Org. Biomol. Chem.* 7 (2009) 4337–4348.
 - [44] C.G. Fortuna, C. Bonaccorso, A. Bulbarelli, G. Caltabiano, L. Rizzi, L. Goracci, G. Musumarra, A. Pace, A. Palumbo Piccionello, A. Guarcello, P. Pierro, E.A.C. Cocuzza, R. Musumeci, New linezolid-like 1,2,4-oxadiazoles active against Gram-positive multidrug-resistant pathogens, *Eur. J. Med. Chem.* 1 (2013) 533–545.
 - [45] A. Pace, S. Buscemi, N. Vivona, The synthesis of fluorinated heteroaromatic compounds. Part 1. Five-membered rings with more than two heteroatoms. A review, *Org. Prep. Proc. Int.* 37 (2005) 447–506.
 - [46] S. Buscemi, A. Pace, A. Palumbo Piccionello, N. Vivona, Synthesis of fluorinated first generation starburst molecules containing a triethanolamine core and 1,2,4-oxadiazoles, *J. Fluor. Chem.* 127 (2006) 1601–1605.
 - [47] I. Pibiri, A. Palumbo Piccionello, A. Calabrese, S. Buscemi, N. Vivona, A. Pace, Fluorescent Hg²⁺ sensors: synthesis and evaluation of a Tren-based starburst molecule containing fluorinated 1,2,4-Oxadiazoles, *Eur. J. Org. Chem.* (2010) 4549–4553.
 - [48] A. Palumbo Piccionello, A. Guarcello, A. Calabrese, A. Pibiri, A. Pace, S. Buscemi, Synthesis of fluorinated oxadiazoles with gelation and oxygen storage ability, *Org. Biomol. Chem.* 10 (2012) 3044–3052.
 - [49] F.S. Palumbo, M. Di Stefano, A. Palumbo Piccionello, C. Fiorica, G. Pitarresi, I. Pibiri, S. Buscemi, G. Giammona, Perfluorocarbon functionalized hyaluronic acid derivatives as oxygenating systems for cell culture, *RSC Adv.* 4 (2014) 22894–22901.
 - [50] H.-L.R. Lee, J.P. Dougherty, Pharmaceutical therapies to recode nonsense mutations in inherited diseases, *Pharmacol. Ther.* 136 (2012) 227–266.
 - [51] P.-I. Ho, K. Yue, P. Pandey, L. Breault, F. Harbinski, A.J. McBride, B. Webb, J. Narahari, N. Karassina, K.V. Wood, A. Hill, D.S. Auld, Reporter enzyme inhibitor study to aid assembly of orthogonal reporter gene assays, *ACS Chem. Biol.* 8 (2013) 1009–1017.
 - [52] S.-W. Jang, C. Lopez-Anido, R. MacArthur, J. Svaren, J. Inglese, Identification of drug modulators targeting gene-dosage disease CMT1A, *ACS Chem. Biol.* 7 (2012) 1205–1213.
 - [53] M. Shalev, J. Kondo, D. Kopelyanskiy, C.L. Jaffe, N. Adir, T. Baasov, Identification of the molecular attributes required for aminoglycoside activity against Leishmania, *Proc. Natl. Acad. Sci. U. S. A.* 110 (2013) 13333–13338.